HOM COUPLER ALTERATIONS FOR THE LHC DQW CRAB CAVITY*

J. A. Mitchell[†1, 2], G. Burt[2], N. Shipman[1, 2], Lancaster University, Lancaster, UK

B. Xiao, S. Verdú-Andrés, Q. Wu, BNL, Upton, NY 11973, USA

R. Calaga, CERN, Geneva, Switzerland

[1]also at CERN, Geneva, Switzerland

[2]also at the Cockcroft Institute, Daresbury, UK

Abstract

As part of the High Luminosity Large Hadron Collider (HL-LHC) project, 16 crab cavities are to be installed in the LHC in 2025. The two crab cavity designs are the Double Quarter Wave (DQW) and Radio Frequency Dipole (RFD). Preliminary beam tests in the Super Proton Synchrotron (SPS) are planned for both cavity types, with the DQW scheduled for testing in 2018. In reference to to Higher Order Mode (HOM) damping, the DQW has three identical on-cell HOM couplers. These HOM couplers provide a band-stop response at the frequency of the fundamental mode and act as a transmission path for the cavity HOMs. For the SPS cavity design, several geometric constraints exist. These give rise to dimensional limitations which in-turn impose limitations on the RF performance of the HOM couplers. As such, for the LHC assembly, the HOM coupler design is re-visited to take into account the relaxed geometric limitations, hence allowing the feasibility of an increased RF performance to be investigated. In addition to the RF performance, several geometric alterations were incorporated to ease manufacturing processes, tolerances and costs.

DQW CRAB CAVITY INTRODUCTION

The purpose of the DQW crab cavity [1] is to provide a transverse electromagnetic kick to a proton bunch, allowing bunch rotation which leads to an increase in luminosity [2]. The effect is applied to both beams prior to collision and a kick of equal magnitude in the opposite direction is then applied after the collisions.

To provide a transverse kick capable of meeting the specified voltage of 3.4 MV [3] whilst fitting in the restricted space available in the LHC, an initial Proof-of-Principle (PoP) DQW was designed. Cavity design alterations were then made primarily to reduce the magnetic field seen at the HOM coupler port areas. Two ports were also removed from the design [4]. The cavity design for the SPS is shown in Fig. 1.

In addition to the fundamental mode at ∼ 400 MHz there also exist several Higher Order Modes (HOMs). Figure 2 shows the on-axis impedance spectrum for the bare cavity up to the beam-pipe cut-off of ∼2 GHz (84 mm beam-pipe) [5]. The simulation was done using CST Microwave Studio [6] with 7.57×10^6 mesh cells and with a wake length of 1 km. In
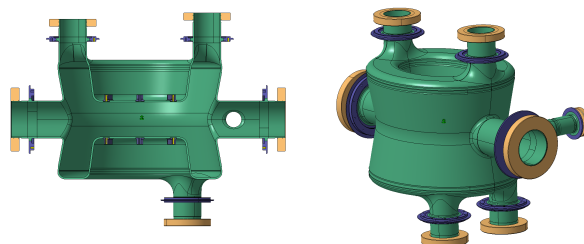
Figure 1: Geometry of the SPS DQW crab cavity.

this paper, the z-direction refers to the longitudinal direction and y to the direction orthogonal to the capacitive plates.
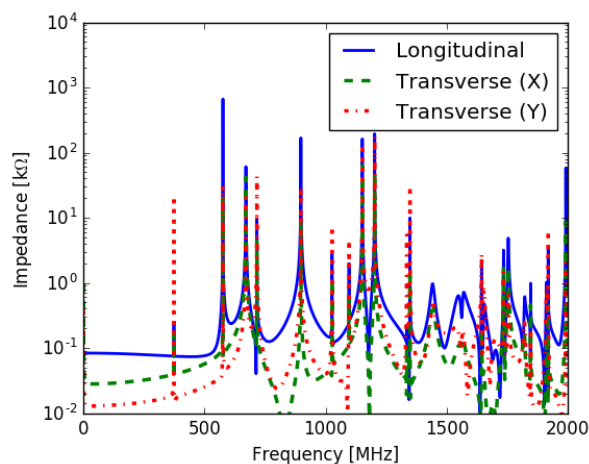

Figure 2: Bare cavity on-axis impedance from wakefield simulations in x, y and z.

HOM couplers are used to damp the HOMs, minimising their effect on beam stability and HOM power. The couplers act as a transmission path to the HOMs but as a band-stop filter to the fundamental mode. The fully dressed cavity is displayed in Fig. 3.

SPS HOM COUPLER

For the SPS crab cavity, geometric limitations meant an angled HOM coupler was designed. A schematic of the coupler is shown in Fig. 4. Although the coupler length restriction imposes restrictions on the RF performance, the right angled coupler gives an advantage in that the ceramic is perpendicular to the direction of field emission. The coupler is made from Niobium and internally cooled with superfluid helium, allowing operation in the superconducting regime.
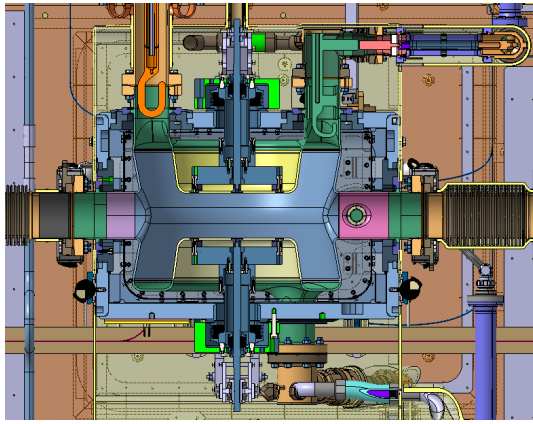
Figure 3: Cross section of the dressed DQW crab cavity fixed in the SPS cryomodule.

The HOM couplers for the DQW are on-cell couplers meaning strong coupling can be achieved to the cavity field, but heating effects are potentially problematic due to the high magnetic field levels of ~45 mT on the hook at the operating voltage of 3.4 MV.
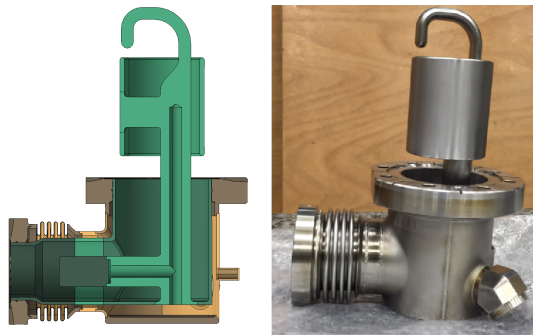

Figure 4: CAD model (left) and photograph (right) of the HOM coupler for the SPS DQW crab cavity.

RF Design

With reference to RF operation, the hook section of the coupler is designed to couple to the field in the cavity. The hook geometry is perpendicular to the direction of magnetic field, providing strong magnetic coupling. Close to the hook is a capacitive jacket connected to the inner conductor of the coupler with a stub section. This acts as an LC band-stop circuit where the jacket dominates the capacitance and the stub the inductance. Capacitive and inductive effects of other geometries, e.g. the capacitance of the hook with the outer wall, also contribute the the stop-band frequency, however their weighting is far reduced compared to that of the 'stub-and-jacket'. This band-stop filter is designed to be centred around the fundamental frequency with a large bandwidth (16.8 MHz at -100 dB) to compensate for changes in the fundamental frequency or manufacturing errors of the HOM coupler. The rest of the coupler then acts as a transmission line where attenuation varies with frequency. High transmission points are seen and denoted as the 'filter interaction

regions'. To optimise the coupler for good transmission of high impedance HOMs, the filter interaction regions are moved in the frequency domain by changing the geometry of the transmission line and right angle bend sections.

Figure 5 displays the coupler's S_{21} from 0–2 GHz. For single coupler simulations, one port lies on the coaxial line after the bend and the other on the open cylindrical waveguide section above the hook. This simulation gives an arbitrary representation of amplitude as the fields decay in the vacuum section of waveguide between the hook and waveguide port. However, for optimisation, having the wave-guide at a fixed height above the coupling element gives a valid point of transmission comparison with a fast simulation time.
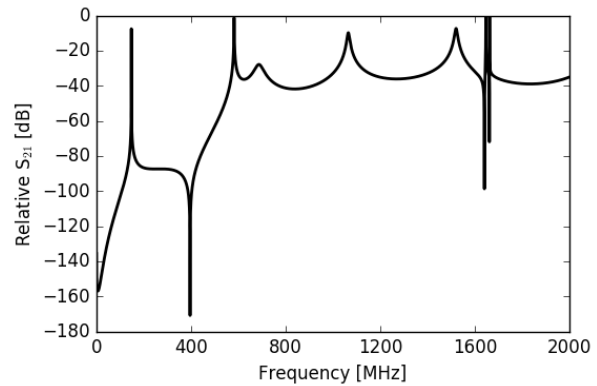

Figure 5: Transmission characteristics of the SPS DQW HOM coupler.

Evaluation of mode impedance can be calculated by doing either a wakefield simulation of the dressed cavity or calculating the R/Q and Q-factors using eigenmode simulations. For the dressed cavity, the amplitude of the impedance from the wakefield simulations can not be taken as accurate due to the high computing time required for convergence of high-Q cavities. Additionally, any modes of extremely high Q-factor may not be visible at all.

For eigenmode simulations, the R/Q values for all axes are calculated. From this, the impedance in each direction can be evaluated (Eq. 1 to Eq. 4), assuming $Q_{ext} \sim Q_L$.

Impedance Calculations

The following formulae and schematics, derived from the Panofsky-Wenzel theorum [7], show how the transverse impedance was calculated.

$$(R/Q)_{\perp(x,y)} = \frac{1}{2\omega U} \cdot \left(\frac{c}{\omega} \left| \frac{dV_z}{d(x,y)} \right| \right)^2 \quad (1)$$

$$R_{\perp(x,y)} = (R/Q)_{\perp(x,y)} \cdot Q_{ext} \cdot \frac{\omega}{c} \quad (2)$$

For longitudinal impedance, the following calculations are applied:

$$(R/Q)_z = \frac{1}{2\omega U} \cdot |V_z|^2 \quad (3)$$

$$R_z = (R/Q)_z \cdot Q_{ext} \qquad (4)$$

For the DQW crab cavity, the voltage points needed for the transverse impedance calculations are shown in Fig. 6. The voltages were taken at $d = \pm 5$ mm in both x and y directions as linearity can be assumed this close to the axis. However, it should be noted that the radial field variation is not linear over the beam pipe radius. The radial voltage for three dominant mode types is therefore plotted to illustrate this point. Following this, the resulting impedance values from 0–2 GHz are plotted in Fig. 7. The eigenmode simulations were performed taking into account the damping effects of the three HOM couplers in addition to the pick-up probe.
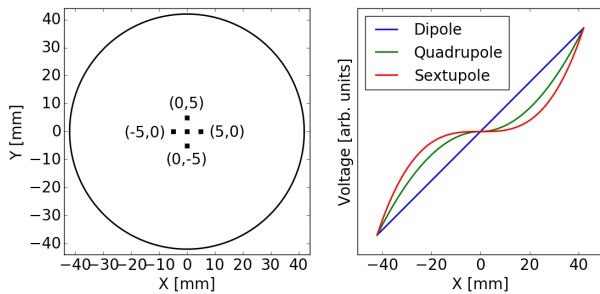

Figure 6: Plots showing the points at which the longitudinal voltages were taken (left) and examples of radial voltage distributions for various mode types (right).
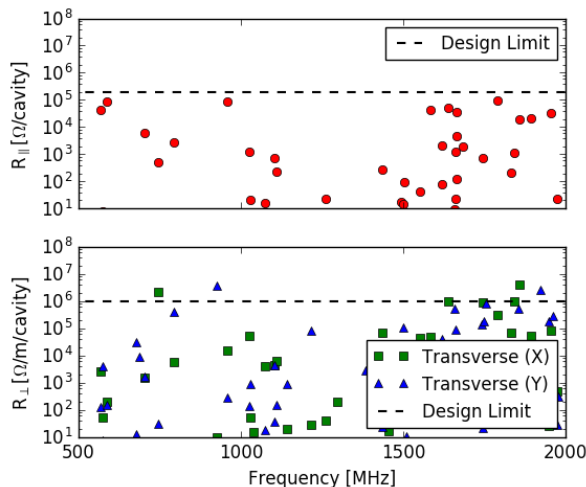

Figure 7: Mode impedance of the SPS crab cavity with SPS HOM couplers.

In terms of damping, there are still large impedance modes at 774 and 928 MHz. Any modifications of the coupler should aim to reduce the impedance of these modes. An upper limit of 1 MΩ/m/cavity for transverse impedances was imposed and 200 kΩ/cavity for longitudinal modes. Additionally, there is a mode at 1.75 GHz which is not damped by the HOM couplers but is instead damped by the pick-up probe. It would be of benefit to design a coupler which could also damp this mode.

Manufacturing Issues

From the experience gained at CERN regarding the manufacture of the couplers, there are three main issues to resolve. Discussions with mechanical engineers at CERN resulted in solutions for each problem.

Problems

1. The section joining the jacket to the stub (Fig. 4) is very difficult to weld due to access restraints, curvature and thickness.

2. Circular cross sections with blended areas can prove difficult to machine to tolerance.

3. The Niobium jacket surrounding the bend section of the coupler (Fig. 4) is very expensive to manufacture as it needs to be machined from one piece of Niobium.

Mitigations

1. A flat section on the capacitive jacket.

2. Rectangular profile with rounded edges.

3. Larger distance from the inner conductor bend to the end of the Niobium shell.

A PROPOSED DESIGN

Design Alterations

Several geometric alterations were applied to the coupler and their effect on high frequency transmission characteristics weighted. Examples of some of the initial design alterations are shown in Fig. 8. For each of these, parametric sweeps were carried out on the modified area and the frequency and amplitudes of the band-stop and filter interaction regions were tracked. Weighting factors could then be allocated to each geometry for optimisation.

The chosen design changes consisted of a, b, c and e shown in Fig. 8. Firstly, the coupler now had a flat section on the capacitive jacket to reduce complications associated with welding. Rectangular cross sections throughout meant simpler machining, a constant profile thickness and a stub induction variation which is not inhibited by the shaft width. Finally, the 'elbow' was raised allowing extrusion of the outer Niobium jacket.

Initially, the stop-band frequency was tuned using the dependence of the stub height on inductance and distance of the flat section of the jacket from the central shaft to control the capacitance. After the stop-band tuning, the two elements were moved independently to observe their respective effects on the frequency from a nominal position, Fig. 9.

Following tuning of the notch frequency, an array of parameters were swept in order to quantify their effect on the operational characteristics of the coupler. The performance
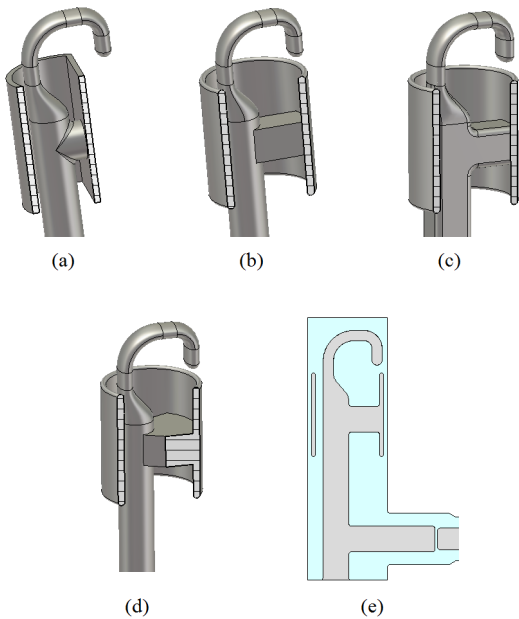
Figure 8: Examples of the alterations made to the SPS HOM coupler for investigation into their effect on RF performance.

Figure 10: Examples of three of the ten values monitored with a control parameter (the height of the inductive stub).
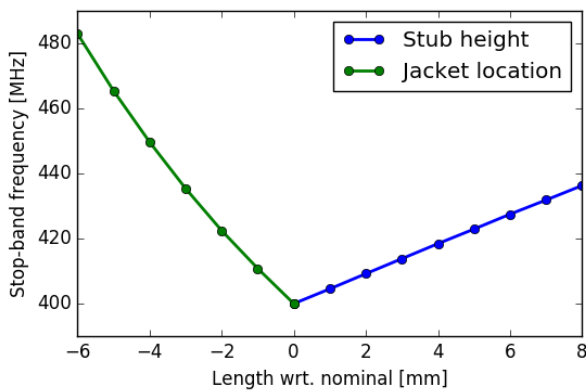

Figure 9: The effect of altering the stub and capacitive jacket on the stop-band frequency.

characteristics monitored were the frequency of the stop-band (notch), bandwidth of the stop-band and the frequencies and amplitudes of the iteration regions (4 in total: IR1, IR2, IR3 and IR4). The interaction regions refer to the four peaks in Fig. 5. An example showing the effect of a variation of the height of the rectangular stub is shown in Fig. 10 for three of the ten S_{21} performance characteristics monitored.

Optimised Version

Using the geometric weighting factors gained from the studies shown in Fig. 10 the filter interaction regions were manipulated in order to preferentially damp the modes which presented a high on-axis impedance. Hence for design purposes, the bare cavity impedance spectrum was plotted over the coupler S_{21} response when optimising. Although the coupler geometry changes the frequency of some modes, overlaying the bare-cavity impedance spectrum like this pro-
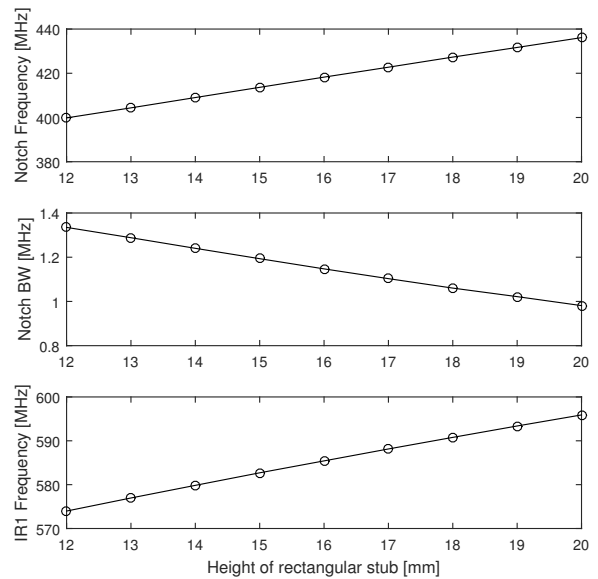
vided a visual basis of where the high transmission areas should be located.

The coupler was then simulated on the cavity and the mode impedances calculated. The results are shown in Figure 11.
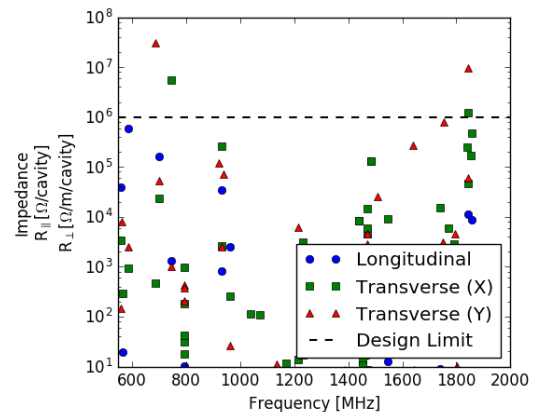

Figure 11: Mode impedance of the SPS DQW with the initial version of the HOM coupler re-design.

From the results it was clear that, although the response at 928 MHz was improved, the impedance of the two modes around 700 MHz had increased and low frequency longitudinal modes had risen above their design limit. As such the transmission at these frequencies needed to increase. Hence the filter interaction regions were moved and the eigenmode simulation was repeated until the design limits were met.

The design criteria was met for each mode apart from one at 1920 MHz which has a transverse-y impedance of 2.16 MΩ/m/cavity. The final transmission response can be seen in Fig. 12, the mode impedances in Fig. 13 and the coupler design in Fig. 14. For the 1920 MHz mode, the

design limit is a limit at a lower frequency. As this limit increases with frequency, this mode impedance is justified at its current impedance level. However, this mode should be investigated to conclude on whether it is possible to achieve adequate coupling.

Referring to the transmission response, the initial interaction region peak is less sharp than the SPS DQW HOM coupler design, and lower in frequency. This means less reduction in damping is seen with a detrimental frequency change of the initial HOMs. However, this comes at the expense of the stop-band bandwidth which is 8.6 times smaller than the SPS design. The bandwidth at -80 dB from the relative measurement is 18 MHz however, and the feasibility of tuning to the correct frequency is much simpler with the rectangular cross-section.

With regards to the 1.75 GHz mode referenced earlier, simulations which did not take into account the damping effects of the pick-up probe showed that this mode was still of high impedance. To damp this mode with the HOM couplers, the port locations wound need to change to allow coupling to this mode.
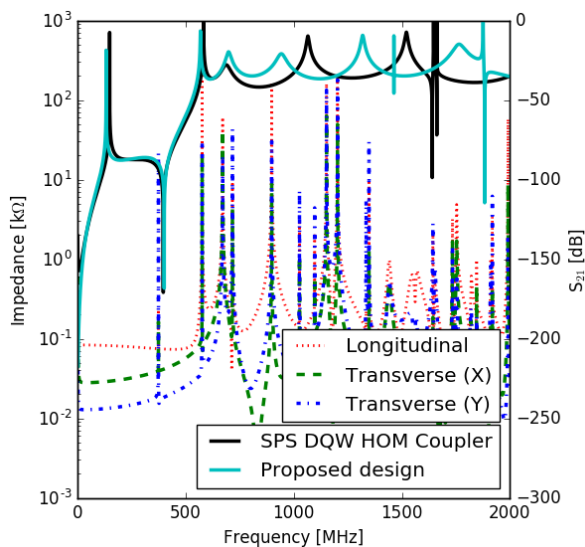

Figure 12: Plot showing the S_{21} from 0–2 GHz for the SPS and re-designed HOM coupler. The bare-cavity impedance spectrum is also plotted for reference.

CONCLUSION AND PROGRESSION

By altering the DQW HOM coupler with geometries which solved the manufacturing issues and logging their effect on RF performance, a HOM coupler was designed which allowed easier manufacture and improved spectral damping.

Future work will include benchmarking the eigenmode simulations in other electromagnetic simulation software and to investigate damping of the mode at 1920 MHz. Following the spectral impedance verification, thermal and multipacting simulations will characterise coupler operation with field level.
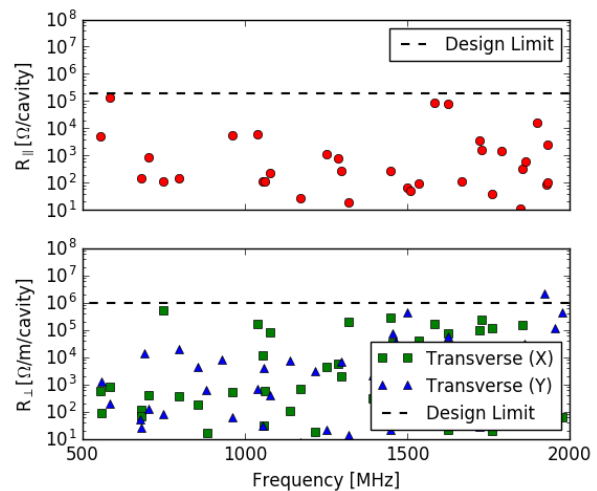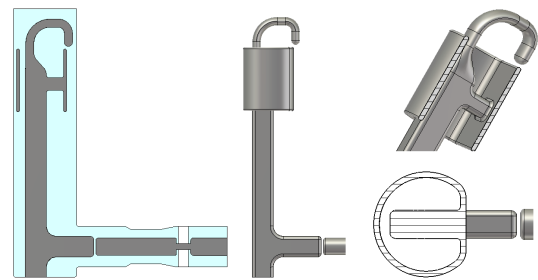

Figure 13: Final mode impedance values.

Figure 14: Proposed HOM coupler design for the DQW crab cavity for HL-LHC upgrade.

REFERENCES

[1] R. Calaga, S. Belomestnykh, J. Skaritka, Q. Wu, and B. Xiao, "A double quarter-wave deflecting cavity for the LHC," in *Proc. IPAC2013*, Shanghai, China, paper WEPWO047, pp. 2408-2410.

[2] R. Calaga, "Crab cavities for the LHC upgrade," No. 2, Proceedings of Chamonix 2012 workshop on LHC Performance, 2012.

[3] O. Bruning and L. Rossi, *The High Luminosity Large Hadron Collider: The New Machine for Illuminating the Mysteries of Universe*, vol. 1. Switzerland,Geneva: World Scientific, 2015.

[4] S. Verdú-Andrés, J. Skaritka, Q. Wu, and B. Xiao, "Optimization of the double quarter wave crab cavity prototype for testing at SPS," in *Proc. SFR2013*, Paris, France, paper THP041, pp. 995–997.

[5] R. Calaga and B. Salvant, "Comments on Crab Cavity HOM Power," tech. rep., CERN, 2015.

[6] Computer Simulation Technology, CST STUDIO SUITE, Bad Nauheimer Str. 19, D-64289 Darmstadt, Germany, http://www.cst.com.

[7] H. Padamsee, J. Knobloch, and T. Hays, *RF Superconductivity for Accelerators*. Wiley,Weinheim, 2008.